Asian Journal of Applied Chemistry Research

Volume 13, Issue 3, Page 1-14, 2023; Article no.AJACR.99172
ISSN: 2582-0273

Green Synthesis of Silver and Zinc Oxide Nanoparticles Using Post-harvest Leaves of *Vigna subterranean* and their Antimicrobial, Anti-inflammatory and Antioxidant Potentials

Adaora Stella Ogbuagu [a*], Lilian Chinelo Innocent [b], Nkeoma Nkasi Okoye [a], Sophina Ogonna Umeh [c] and Josephat Okechukwu Ogbuagu [a]

[a] Department of Pure and Industrial Chemistry, Nnamdi Azikiwe University, Awka, Nigeria.
[b] Department of Chemistry Education, College of Education Technical Umunze, Anambra State, Nigeria.
[c] Department of Applied Microbiology and Brewing, Nnamdi Azikiwe University Awka, Anambra State, Nigeria.

Authors' contributions

This work was carried out in collaboration among all authors. All authors read and approved the final manuscript.

Article Information

DOI: 10.9734/AJACR/2023/v13i3243

Open Peer Review History:
This journal follows the Advanced Open Peer Review policy. Identity of the Reviewers, Editor(s) and additional Reviewers, peer review comments, different versions of the manuscript, comments of the editors, etc are available here: https://www.sdiarticle5.com/review-history/99172

Original Research Article

Received: 18/02/2023
Accepted: 20/04/2023
Published: 24/04/2023

**Corresponding author: Email: as.ogbuagu@unizik.edu.ng;*

ABSTRACT

Green route synthesis of nanoparticles has been known to be beneficial as one of the non-toxic methods of synthesizing potential drugs. The aqueous extracts of *Vigna subterranean* (Bambara nut) leaves discarded after harvest were used in the synthesis of silver and zinc nanoparticles using 1mM concentration of silver nitrate ($AgNO_3$) and zinc oxide (Zn O) respectively. The nanoparticles were characterized using Ultraviolet-Visible (UV/Vis) Spectroscopy, Fourier-Transform Infrared Spectroscopy (FT-IR), Scanning Electron Microscopy (SEM) and X-ray Diffraction Analysis (XRD). Antibacterial and antifungal studies were conducted on two strains of bacteria (*Salmonella typhi. and Staphylococcus aureus*) and two strains of fungi *(Aspergillus niger and Aspergillus flavus*) based on their inhibition zone diameter using paper disk diffusion methods. Anti-inflammatory and antioxidant studies were also conducted on the nanoparticles using the inhibition of protein denaturation and reduction of DPPH respectively. The λmax absorption of the nanoparticles were found to be 434 and 460 nm respectively in the UV/Vis region. Their shapes and nature were spherical and amorphous as confirmed by the SEM and XRD analysis. The diameters of the nanoparticles ranged from 20 to 60 nm using the Particle metric particle analysis software. The FTIR confirmed the presence of some bioactive functional groups involved in the reduction of $AgNO_3$ and Zn O to Ag and Zn nanoparticles. The nanoparticles showed moderate activities against the tested bacterial strains while showing no activity against the fungi strain when compared with standard drugs. They however showed strong anti- inflammatory and antioxidant activities. The silver and zinc mediated nanoparticles could serve as a potential source for antioxidants and anti-inflammatory drugs.

Keywords: Green synthesis; nanoparticles; anti-inflammatory; antioxidant.

1. INTRODUCTION

Nanotechnology has emerged as intriguing area of study due to its vast application in diverse fields such as adsorption, optical sensor, catalysis, water treatment, drug delivery and nano-medicine [1]. It originated from various fields of science and engineering where interestingly, new ideas have been utilized to alter molecules and single atoms [2]. It provides the ability to engineer the properties of materials by controlling their size and this has driven research toward a multitude of potential uses for nanomaterials [3]. Nanotechnology is significant on account of its dominance upon the understanding, use and control of matter at magnitudes of a minute scale, akin to approaching atomic levels, with which to manufacture new substances, instruments and framework [4]. In the rapidly improving field of nanotechnology, nanomaterials are on the prominent application in environmental and medical sciences. Nanomaterials are the leading requirement of the rapidly developing field of nano-medicine and bio-nanotechnology. Biosynthesis of nanoparticles by plant extracts is currently under exploration [5]. The bio-reduction of metal nanoparticles by a combination of bio-molecules found in plant extracts such as enzymes, proteins, amino acids, vitamins, typically obtained by contact of broth of plant with metal salts has been intensively investigated in recent years [6]. These studies include the use of the various parts of plant in the synthesis of metal nanoparticles [7], the antibacterial potentials of Ag nanoparticles [8], the antifungal and the antiproliferative studies [9] and the toxicological and anti-dermatophytic activities among others [10] This method of synthesis is known as green synthesis and it provides advancement over chemical and physical methods as it is cost effective, environment friendly, and there is no need to use toxic chemicals, high temperature, high pressure and energy [11].

Vigna subterranean is a legume that originated from West Africa and is cultivated across the semi-and sub-Saharan Africa but has become widely distributed throughout the semi-arid zone of sub-Sahara Africa [12]. It is a member of the family Fabaceae, which is also named as bean family, legume or pulse family. It is also known with many local names in different parts of the world; Bambara nut, Bambara groundnut, Bambara bean, Congo goober, Earth pea, Hog-peanut or Ground bean. It is cultivated principally by farmers as a famine crop due to its agronomic values and the ability to produce in soils that are considered insufficiently fertile for cultivation of other more favoured species such as common beans and groundnuts [13]. It is cultivated for its

subterranean pods and produces reasonable yields even under conditions of drought and low soil fertility. It is a hardy crop and has been recognized as an important nutritious food source when food is scarce, it possesses the abundance of both essential and nonessential amino acids as well as phytochemicals such as alkaloids, saponins, flavonoids and tannins [14,15]. The drought resistance of *V. subterranean* could be attributed to its climate-smart features including its ability to fix nitrogen [16,17] and to grow under adverse environmental conditions. Aside its use as a staple food and fodder for livestock as well as in soil reclamation, there are no other use for it and this study seeks to find the use of the matured (post-harvest) leave in nanoparticle synthesis.

2. MATERIALS AND METHODS

2.1 Materials

The materials used for this biosynthesis include: *V. subterranean* leaves*, Staphylococcus aureus GB688GB668, Salmonella typhi NCTC 83288832, Aspergillus nigreniger KF 908788, Aspergillus flavus KP 770981, KP770981,* Nutrient Agar, Mueller Hinton Agar, Potato Dextrose Agar, ciprofloxacin, fluconazole,2, 2-diphenyl-2-picrylhydrazyl (DPPH), Bovine serum albumin,, silver nitrate, zinc oxide, KBR, HCl, Whatman filter paper.

2.2 Sample Collection and Preparation

The seeds of *V. subterranean* were planted in Umunze, Anambra state, Nigeria. They were harvested after sixteen weeks. The leaves were collected and washed running tap water and later with distilled water. They were dried in an electric oven at a temperature of 35^{o}C for 48hours. They were pulverized using electric kitchen blender *(Bina tone Mode*l *BLG 450*), weighed and stored in air tight containers protected from sunlight and atmospheric moisture for further use.

The test bacteria *Salmonella typhi (S. typhi) and Staphylococcus aureus (S. aureus)* and fungi *Aspergillus niger (A. niger)* and *Aspergillus flavus (A. flavus)* were obtained from the Research laboratory, Department of Applied Microbiology and Brewing, Nnamdi Azikiwe University, Awka, Anambra State, Nigeria. They were sub cultured and characterized to confirm their identity and stored in bijou slants in refrigerator maintained at 4^{o}C.

2.3 Preparation of Plant Extracts

The aqueous leaves extract of *V*. *subterranea*n was prepared by measuring 25g of the samples into a 500mL flask and adding 200mL of water. This was heated in a water bath for 20 minutes at 80^{o}C. The extract was then allowed to cool for twenty minutes and filtered off three times with filter papers removing the organic residue. The extract was used for the synthesis of silver and zinc nanoparticles.

2.4 Synthesis of Silver and Zinc Nanoparticles

A 10 ml portion of the extract was added into 90ml of 0.01M of aqueous silver nitrate, $AgNO_3$ solution in a 500mL glass beaker. It was gradually and continuously stirred using a spatula and heating on a hotplate at 80^{o}C for 30 minutes within which a color change from brown to deep red and then to a lighter color showing a complete reduction. The silver nanoparticle solutions of extract were allowed to stand for 24 hours after which the nanoparticles settled at the bottom of the flask. This solution was then decanted and the supernatant eliminated and the residue was centrifuged and these particles were then dried in an oven at 80^{o}C and then stored in a container for characterization and other analyses. The same procedure was used for zinc nanoparticles using the same volume and concentration as used in the synthesis of Ag nanoparticles but in this case, zinc oxide was used in the place of silver nitrate.

2.5 Characterization of Synthesized Silver and Zinc Nanoparticles

1. UV-visible spectroscopy analysis

The bio-reduction of the silver ion and zinc ion in aqueous solution were measured by sampling 1 ml aliquot of the samples compared with 1 ml of distilled water used as a blank, and subsequently measuring the UV-visible spectrum of the solution. UV-visible spectrum of the solutions was monitored on Cary Series UV-vis Spectrophotometer Agilent Technology, operated within the wavelength range of 200 to 800 nm.

2. FT-IR spectroscopy analysis

Fourier Transform Infrared Spectroscopy, Perkin Elmer- RXI Version 10.03.09 spectrophotometer was used to perform analysis on the samples

and investigate the functional groups involved in the formation of silver and zinc nanoparticles by comparing the spectra of the sample of leaves and roots extract and that of the synthesized silver and zinc nanoparticles.

3. Scanning Electron Microscope (SEM)

The morphology and shape of the synthesized silver and zinc nanoparticles were studied using SEM.

4. X-ray diffraction analysis (XRD)

XRD (PAN analytical, Netherlands) patterns were obtained with a diffractometer (Empyrean model, Netherlands) operated at a voltage of 45 KV and a current of 40 mA using Cu-Kα radiation of wavelength of 1.541 A.

2.6 Antimicrobial Analysis

The antibacterial activity of the synthesized silver nanoparticles and zinc nanoparticles was determined using a disc diffusion method. The test bacteria *Salmonella typhi (S. typhi) and Staphylococcus aureus (S. aureus)* and fungi *Aspergillus niger (A. niger)* and *Aspergillus flavus (A. flavus)*.

The required quantities of dehydrated Nutrient Agar, Potato Dextrose Agar and Mueller Hinton Agar were separately weighed and prepared with distilled water according to the manufacturer's specifications. Gentle heating was applied to aid dissolution; the media was then sterilized by autoclaving at 121^{o}C for 15minutes. The media was used aseptically for the assay. Discs of 6mm diameter were punched out from Whatman filter paper with the aid of paper puncher and placed into containers; the discs were then sterilized in a laminar flow using a UV light ray. The sterile paper discs were then impregnated with different concentration of Zinc and Silver Nanoparticles for the assay.

The antibacterial activities of Zinc and Silver Nanoparticles were evaluated by agar disk diffusion method (6mm) using Mueller Hinton Agar. 0.1ml of Bacterial suspension (*Salmonella typhi. and Staphylococcus Aureus*) each was inoculated on Mueller Hinton agar plates. The 6mm diameter disk was impregnated with respective concentrations of Zinc and Silver nanoparticles (100mg/ml, 50mg/ml and 25mg/ml) and labeled 10^{-1}, 10^{-2} and 10^{-3}, respectively and then allowed to dry. Thereafter, the disks were picked with sterile forceps and placed on the inoculated agar plates under strict aseptic conditions. Ciprofloxacin was used as control. All the plates were incubated at 37^{o}C for 24 hr. Microbial growth was determined by measuring the diameter of the zone of inhibition using a transparent millimeter ruler.

Antifungal activities were evaluated by agar disk diffusion method (6mm) using Potato Dextrose Agar. Standardized inoculum of the isolated fungi *(Aspergillus niger and Aspergillus flavus*) was spread onto the surface of plates. 0.1ml of different concentrations (100mg/ml, 50mg/ml and 25mg/ml) of zinc and silver nanoparticles were separately introduced onto the disc and allowed to dry. Thereafter, the disks were picked with sterile forceps and placed on the inoculated agar plates under strict aseptic conditions. Fluconazole was used as control. All the plates were incubated at room temperature for 48 and 72 hours. Zones of inhibition were measured using a meter rule recorded in millimeters for each concentration which were the average length and width of the cleared portion around each paper disc.

2.6.1 Anti-inflammatory analysis

This analysis was conducted using the inhibition of protein denaturation. Bovine serum albumin (BSA) was used as a test material for this analysis. 2ml of 1% aqueous solution of Bovine albumin fraction was mixed with 400uL of synthesized silver nanoparticles and zinc nanoparticles concentrations separately and the pH of reaction mixtures was adjusted to 6.8 using HCl. The reaction mixture was then incubated at room temperature for 20minutes in a water bath. The mixture was cooled to room temperature and the absorbance value was measured spectrophotometrically at 660 nm. An equal amount of the nanoparticles was replaced with Acetylsalicylic acid and taken as a positive control. The experiment was performed in triplicate. Percent inhibition of protein denaturation was calculated as follows:

$$\% \text{ inhibition} = (A_{blank} - A_{sample} / A_{blank}) \times 100$$

Where A_{blank} is the absorbance of the control reaction (containing all the reagents except the test compound) and A_{sample} is the absorbance of the test compounds.

2.6.2 Antioxidant analysis

Free radical scavenging 2,2-diphenyl-2-picrylhydrazyl (DPPH) assay was used for the

evaluation of the antioxidant capacity of the synthesized nanoparticles.

To assess the scavenging ability on DPPH, each synthesized silver and zinc nanoparticles (5-20mg/ml) in water will be mixed with 1 ml of methanol solution containing DPPH radicals (0.2mM). The mixture was shaken vigorously and left to stand for 30min in the dark before measuring the absorbance at 517 nm against a blank. Then the scavenging ability was then calculated using the following equation:

$$\% \text{ inhibition} = (A_{blank} - A_{sample} / A_{blank}) \times 100$$

Where A_{blank} is the absorbance of the control reaction (containing all the reagents except the test compound) and A_{sample} is the absorbance of the test compounds.

3. RESULTS AND DISCUSSION

3.1 Formation of Silver and Nanoparticles

The aqueous leaves extract of *V. subterranean* were used to synthesize silver and zinc nanoparticles respectively and the formation of nanoparticles was evident from the color change of the leaves extract from brown to reddish brown upon addition of $AgNO_3$ and ZnO solutions and heating for 30 minutes with continuous stirring. This color change indicated the reduction of silver (I), Ag^+ to metallic silver Ag^0 and Zn^{2+} to Zn^0 respectively. In a period of two hours, the colour of the solutions stopped changing after getting to a lighter shade further suggesting the complete bio-reduction of $AgNO_3$ into Ag nanoparticles and ZnO into Zn nanoparticles respectively. Similar color formations were reported in the literature [18,19,20].

3.2 UV-visible Spectroscopy

The UV-visible spectral analysis of leave extracts of V. *subterranean* mediated silver and zinc nanoparticles within the range of 200nm – 800nm showed continuous absorption in the visible range. [21] obtained similar UV-visible spectra for amorphous iron nanoparticles synthesized using flower extracts of *Piliostigma thonningii*. The UV-visible spectral analysis of the leaves extracts of *V. subterranean* mediated nanoparticles gave a maximum absorbance peak near 440nm as shown in Fig. 1 indicating the formation of nanoparticles. Silver nanoparticles give a peak in a range of 450nm-500nm [22]. The wavelength obtained is in conformity with the wavelength obtained in the work of [19] varied slightly to the peak value of in the work carried out by [22], at 460nm and [23] at 434nm.

The synthesized zinc nanoparticle mediated from leaves extracts of *V. subterranean* showed UV peaks recorded by the spectrophotometer. The maximum absorption peaks of zinc nanoparticles synthesized from leaves extract was recorded at 440nm as shown in Fig. 2, this further verified the formation of zinc nanoparticles. This result satisfies standard zinc oxide absorption pattern because all oxides of materials have wide band gaps and then have shorter wavelengths and if the material is at nanoscale, it tends to have further shorter wavelength [20]. The wavelength obtained is in agreement with the wavelength obtained in the work of [19] varied slightly to the peak value of in the work carried out by [22], at 460nm and [23] at 434nm.

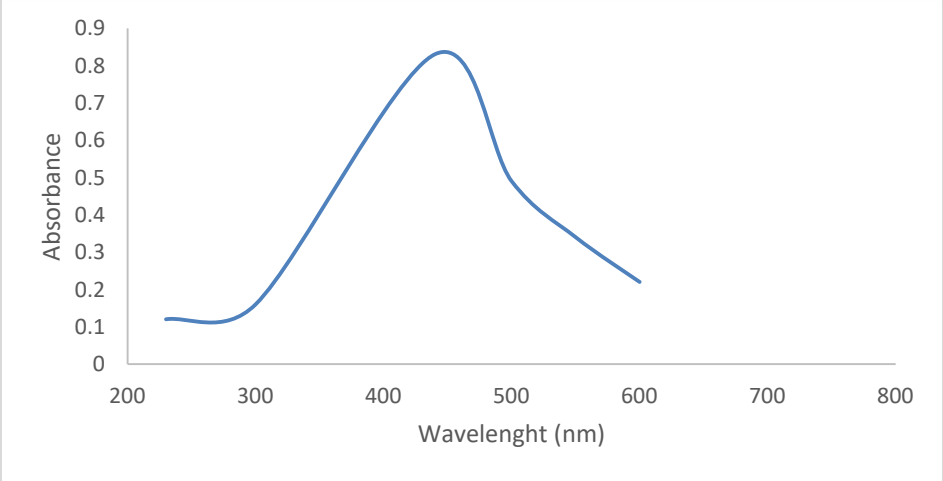

Fig. 1. UV-Visible absorption spectrum of leaves silver nanoparticles

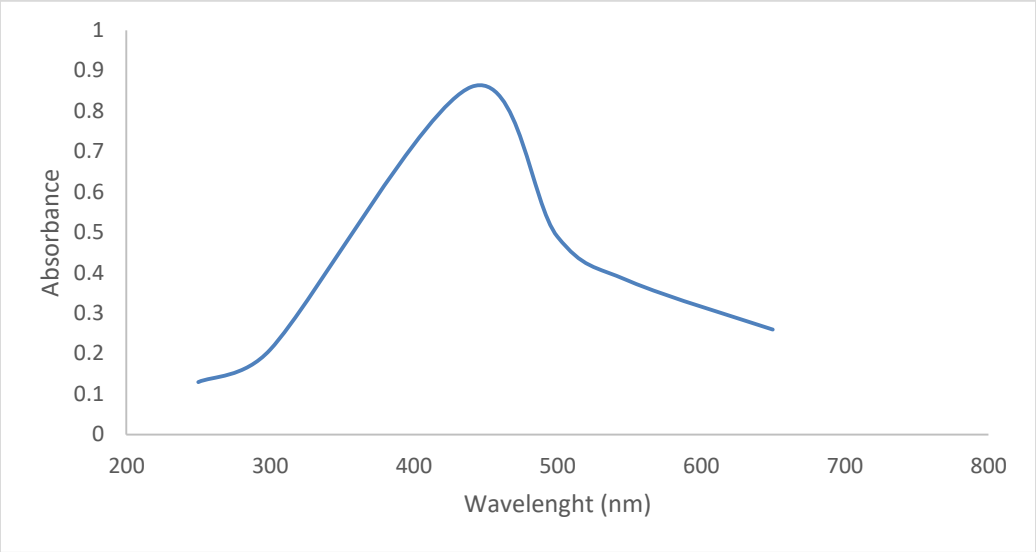

Fig. 2. UV-Visible absorption spectrum of leaves zinc nanoparticles

Table 1. FT-TR spectra data obtained for the silver nanoparticles

Peaks (cm^{-1})	Functional Groups	Intensities
1013.84	C-O stretch due to alcohols	67.62
1319.48	O-H bend due to tert-alcohol or phenol	83.78
1401.48	N-H bend due to amides II	83.71
1617.66	C=C stretch due to conjugated alkene	73.01
2922.23	C-H stretch due to alkane CH_3, CH_2 and CH	89.58,
3272.60	O-H stretching due to alcohol	86.86

3.3 FT-IR Spectroscopy

FT-IR analysis was performed to investigate functional groups present in the synthesized silver and zinc nanoparticles both for the leaves and roots of *V. subterranean*. The spectrum for each of the synthesized nanoparticles is show in Table 1 above:

The FT-IR spectrum of silver nanoparticles of leaves of V. *subterranean* displayed prominent bands at 1013.84cm^{-1}, 1319.48cm^{-1}, 1401.48cm^{-1}, 1617.66cm^{-1}, 2922.23cm^{-1}, 3272.60cm^{-1} which indicate the presence of C-O stretch due to alcohols, O-H bend due to tert-alcohol or phenol, N-H bend due to amides II, C=C stretch due to conjugated alkene, C-H stretch due to alkane CH_3, CH_2 and CH, O-H stretching due to alcohol respectively. The presence of these functional groups in the spectrum is an indication that a chemical change has occurred and theses groups were involved in the bio-reduction of silver ions to silver nanoparticles followed by the stabilization of the silver nanoparticles. The presence of C-O, C=C, C-H and O-H groups in the silver nanoparticles suggested that the surface of the nanoparticles was associated with compounds whose chemical nature comprised of these groups. Also, the O-H group might be as a result of water molecules that adhered to the surface of the silver nanoparticles. This result is in agreement with the results obtained by [21]. The presence of N-H group is from proteins and amino acids and suggests that they could bind to metals and proteins could possibly form a layer around the metal for preventing agglomeration and thereby stabilizing the nanoparticles and this is in agreement with previous report of [20]. The O-H functional group act in capping the synthesized silver nanoparticles and also the capping and reduction of silver nanoparticles by bio-molecules present in leaves as shown in Table 2 could be responsible for prolonged stability [19,8].

Table 2. FT-IR Data obtained for the zinc nanoparticles

Peaks (cm^{-1})	Functional Groups	Intensities
1013.84	C-O stretch due to alcohols	58.54
1401.48	O-H bend due to tert-alcohol or phenol	82.59
1543.12	N-H bend due to amides II	78.38
1625.12	C=C stretch due to conjugated alkene	77.25
2922.23	C-H stretch due to alkane CH_3, CH_2 and CH	87.33
3265.15	O-H stretching due to alcohol	84.19

The FT-IR spectrum of zinc nanoparticles of leave of *V. subterranean* showed prominent bands at 1013.84cm^{-1}, 1401.48cm^{-1}, 1543.12cm^{-1}, 1625.12cm^{-1}, 2922.23cm^{-1} and 3265.15cm^{-1}, which indicates the presence of C-O stretch due to alcohols, , O-H bend due to tert-alcohol or phenol, N-H bend due to amides II, C=C stretch due to conjugated alkene, C-H stretch due to alkane CH_3, CH_2 and CH, O-H stretching due to alcohol respectively. The presence of these functional groups in the FT-IR spectrum indicates that these groups were involved in the bio-reduction of silver ions to silver nanoparticles followed by the stabilization of the silver nanoparticles. The presence of C-O, C=C, C-H and O-H groups in the silver nanoparticles suggested that the surface of the nanoparticles was associated with compounds whose chemical nature comprised of these groups. This result is in agreement with the results obtained in the literature [19,21] Also, the O-H group might be as a result of water molecules that adhered to the surface of the silver nanoparticles. This result is in agreement with the results obtained in the literature [21] The presence of N-H group is from proteins and amino acids and suggests that they could bind to metals and proteins could possibly form a layer around the metal preventing agglomeration and thereby stabilizing the nanoparticles and this is in agreement with a previous report [21]. The O-H functional group act in capping the synthesized silver nanoparticles and also the capping and reduction of silver nanoparticles by bio-molecules present in leaves could be responsible for prolonged stability [19].

3.4 Scanning Electron Microscope (SEM)

SEM images revealed that the synthesized leaves silver nanoparticles were spherical in shape, scattered over the surface and no aggregates were noticed. The diameter of the particles was below 100nm in the range of 20 to 60nm. This result is in conformity with the results of Abdulkadir et. al and Igwe and Nnaemezie [19,22].

The SEM images of the synthesized silver and zinc nanoparticles are shown in the figures below.

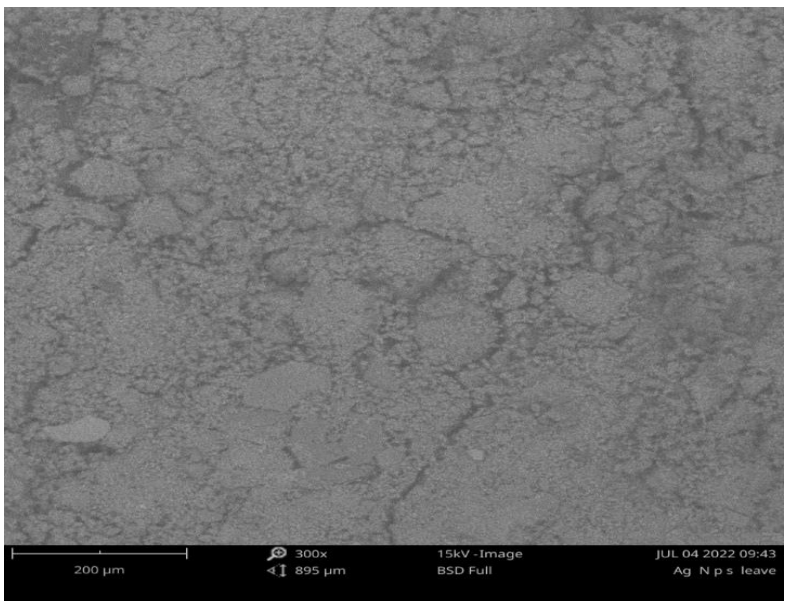

Fig. 3. SEM images of silver nanoparticles synthesized from leaves extracts

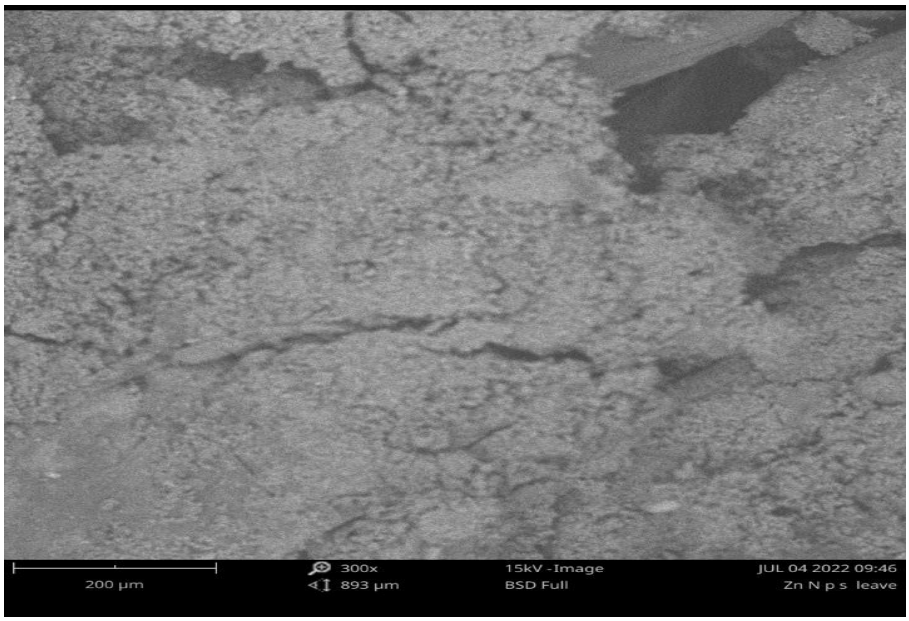

Fig. 4. SEM image of zinc nanoparticles synthesized from leaves extracts

SEM images revealed that the synthesized leaves zinc nanoparticles were spherical in shape, scattered over the surface and no aggregates were noticed. The diameter of the particles was from the range of 30 to 60nm. The difference in the sizes of the nanoparticles is probably due to the fact the nanoparticles were being formed at different times. This result is in conformity with the results of [19,22].

3.5 X-ray Diffraction (XRD)

XRD was used to determine the crystal structure of the synthesized zinc and silver nanoparticles from leaves and roots extracts of *V. subterranean*. The XRD pattern of the zinc and silver nanoparticles of both leaves and roots extract of *V. subterranean* did not have distinct diffraction peaks, suggesting the amorphousness of the synthesized zinc and silver nanoparticles. This had earlier been demonstrated by the UV-visible analysis on the synthesized zinc and silver nanoparticles where continuous absorption in the visible range was observed. The difference in the sizes of the nanoparticles is probably due to the fact the nanoparticles were being formed at different times. This is in agreement with the report of [21] for amorphous iron nanoparticles.

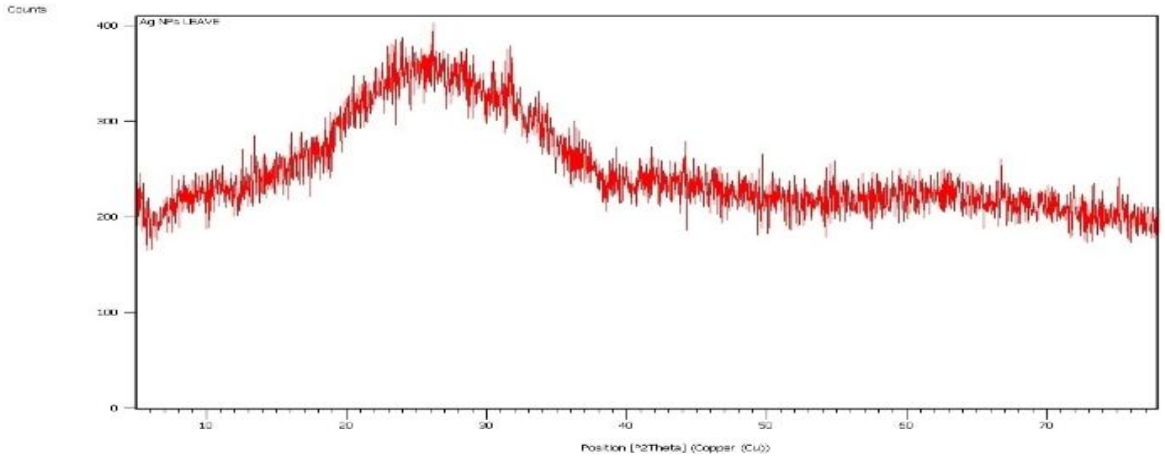

Fig. 5. XRD patterns of silver nanoparticles synthesized using leave extract of *V. subterranean*

The XRD patterns of the silver nanoparticles mediated from leaves extract of *V. subterranean* is shown in Fig. 6.

The XRD patterns of the silver and zinc nanoparticles mediated from leaves extract of *V. subterranean* is shown in Figs. 5 and 6. The XRD patterns lack distinct diffraction peaks, suggesting that both nanoparticles wereare amorphous. In the XRD spectrum of the silver and zinc nanoparticles mediated from leaves extract, broad humps are seen at about 2θ = 25 and this may be attributed to organic materials present in the mixture and the none crystalline nature of the nanoparticles. This result is in conformity with that reported by [21,24] and [25].

3.6 Antimicrobial Analysis

The antimicrobial analysis of zinc nanoparticles and silver nanoparticles were tested to determine the susceptibility of Bacterial and fungal isolates using disc diffusion assay, a modified protocol of Kirby Bauer described by [26] was adapted. Antimicrobial analysis was conducted using the synthesized silver and zinc nanoparticles from leaves extract of *V. subterranean* against bacteria pathogens *Staphylococcus aureus* and *Salmonella typhi* and fungi pathogens *Aspergillus niger and Aspergillus flavus.* The antibacterial analysis was conducted using ciprofloxacin and fluconazole as controls. Ciprofloxacin was used as antibacterial drug while Fluconazole as antifungal drug, all served as control. The results of the analysis is shown in Table 3.

The result of the antimicrobial bioassay was based on the inhibitory zones of the silver and zinc nanoparticles solution in millimeter prepared at different concentrations. For the leaves zinc nanoparticle, the activity of the nanoparticles increased throughout with increasing concentration from 100mg/ml to 25mg/ml and was effective in inhibiting bacterial growth *Staphylococcus aureus* and *Salmonella typhi*. In each case of inhibition of bacterial growth, the control ciprofloxacin drug was more active than

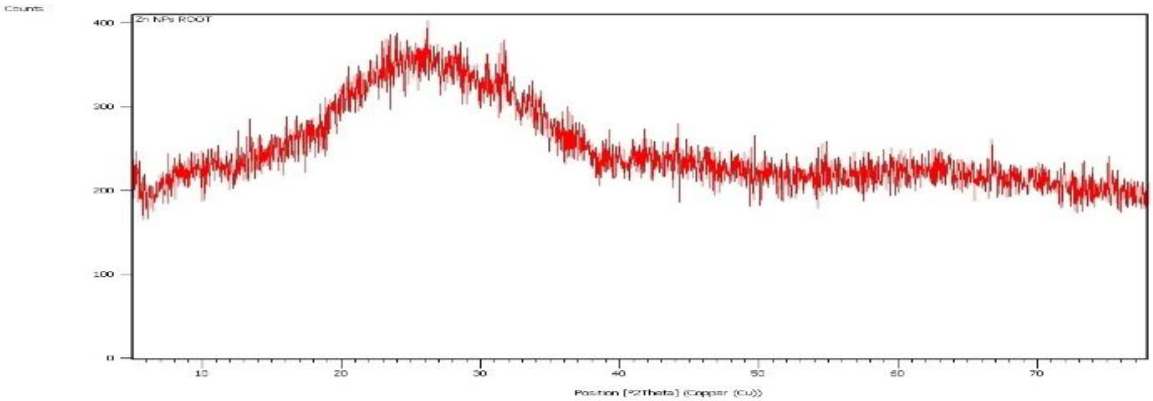

Fig. 6. XRD patterns of zinc nanoparticles synthesized using leaves extract of *V. subterranean Subterranean*

Table 3. Antimicrobial activity of zinc and silver nanoparticles against test organisms

Sample ID	Zones of inhibition (mm) produced by the dilutions of Zinc, Silver nanoparticles and control antibiotics on the test organisms											
	Salmonella typhi			*S. aureus*			*A. niger*			*A. flavus*		
	10^{-1}	10^{-2}	10^{-3}	10^{-1}	10^{-2}	10^{-3}	10^{-1}	10^{-2}	10^{-3}	10^{-1}	10^{-2}	10^{-3}
Zinc leaves	28	25	24	27	24	23	NA	NA	NA	NA	NA	NA
Silver leaves	18	17	17	21	19	15	NA	NA	NA	NA	NA	NA
Ciprofloxacin	51	49	48	70	69	69						
Fluconazole							24	24	23	29	27	24

Key: NA indicates No Activity
S. aureus refers to Staphylococcus Aureus
A. niger refers to Aspergillus niger
A. flavus refers to Aspergillus flavus

the leaves zinc nanoparticles at low concentrations. Zinc leaves nanoparticles were found to show no activity/ inhibition against *Aspergillus niger and Aspergillus flavus*. The nanoparticles showed best activity against *Salmonella typhi* (28mm) as compared to *Staphylococcus aureus* (27mm). And both *Staphylococcus aureus* and *Salmonella typhi* showed minimum inhibitory concentration at 25mg/ml for the synthesized zinc leaves nanoparticles. The difference in activity against these two types of bacteria could be as a result of differences in structure and composition of the cell membrane. Gram-positive bacteria (*Staphylococcus aureus*) have thicker peptidoglycan cell membranes compared to the Gram-negative bacteria (*Salmonella typhi*) and so it would be more difficult for zinc nanoparticles to penetrate it, resulting in a low antimicrobial response [20,21,10].

Silver nanoparticles mediated from leaves extracts showed increased activity throughout with increase in concentration from 100mg/ml to 25mg/ml and was effective in inhibiting bacterial growth of *Staphylococcus aureus* and *Salmonella typhi*. In each case of inhibition of bacterial growth, the control ciprofloxacin drug was more active than the leaves silver nanoparticles at low concentrations. The silver nanoparticles showed no activity/inhibition against *Aspergillus niger and Aspergillus flavus,* however in a study conducted using n hexane extracts of the root of the same plant, a strong activity against the same organism was observed [27]. The nanoparticles showed best activity against *Staphylococcus aureus* (21mm) as compared to *Salmonella typhi* (18mm). And both showed minimum inhibitory concentration at 25mg/ml for the synthesized leaves silver nanoparticles.

3.7 Anti-inflammatory Analysis

The anti-inflammatory analysis was conducted using the inhibition of protein denaturation. The synthesized zinc and silver nanoparticles mediated from leaves extracts of *V. subterranean* was used to test the inhibition of protein denaturation using Bovine Serum Albumin (BSA). The result of the analysis is shown in Table 4.

The silver and zinc nanoparticles mediated from leaves extracts of *V. subterranean* exhibited properties that are comparable with standard DMSO. Protein denaturation is a process by which proteins lose their primary and tertiary structures by application of external stress compounds such as strong acid, base, concentrated inorganic-organic salt or heat [28]. Inflammation is caused by protein denaturation. In the process of inflammation, proteins lose their quaternary structure, thereby inducing aggregation which activates harmful inflammation signs [28]. The inhibition of albumin denaturation by silver and zinc nanoparticles mediated from both leaves and roots extracts of *V. subterranean* indicate anti-inflammatory activities.

The maximum inhibition of protein denaturation was observed in zinc nanoparticles mediated from root extracts (69%) followed by zinc nanoparticles mediated from leaves extract (61.89) all at 100mg/ml concentration. These results showed less inhibition than the standard at 90% inhibition at 100mg/ml concentration. At 25mg/ml concentration, the synthesized silver and zinc nanoparticles showed minimum inhibition of protein denaturation. The anti-inflammatory activity of all the nanoparticles was higher as the concentration of the nanoparticles increased. The leaves silver nanoparticles showed the highest inhibition of protein denaturation of all the synthesized nanoparticles followed by leaves zinc nanoparticles, then roots silver nanoparticles and then roots zinc nanoparticles. This corroborated with the results obtained by Salve et. al and Rangasamy [27,28,29].

Table 4. Anti-inflammatory activity of zinc and silver nanoparticles

Nanoparticles	Concentrations(mg/ml)	% Inhibition
Zinc leaves	100.00	61.89
	50.00	51.00
	25.00	36.00
Silver leaves	100.00	12.78
	50.00	11.11
	25.00	5.56

3.8 Antioxidant Analysis

Free radical scavenging 2,2-diphenyl-2-picrylhydrazyl (DPPH) assay was used for the evaluation of the antioxidant activity of the synthesized silver and zinc nanoparticles. The antioxidant activity of the silver and zinc nanoparticles mediated from leaves and roots extract of *V. subterranean* are shown in the Fig. 7.

For the silver nanoparticles mediated from leaves extract of *V. subterranean,* the synthesized nanoparticles showed scavenging activity against DPPH at different concentrations of 10mg/ml (35.65%), 20mg/ml (62.29%), 30mg/ml (73.63%), 40mg/ml (82.88%), 50mg/ml (87.69%) and 75mg/ml (90.25%). The antioxidant activity was found to be higher as the concentration of the leaves extract of silver nanoparticles increased, with the highest activity 90.25% being at the concentration of 75mg/ml. The presence of the functional group in the phytochemicals present in the leaves of *V. subterranean* results in natural anti-oxidants with high reducing capacity. The mechanism of anti-oxidant activity of silver nanoparticles was by single electron transfer to the DPPH radical the silver nanoparticles have free radical resistive ability due to the antioxidants in the nanoparticles (Fig. 8). It is a possibility from the results obtained that the silver nanoparticles mediated from leaves extract possesses hydrogen-donating capabilities and acts as an antioxidant. This result corroborated with work conducted by Salve et.alfound in the literature [28].

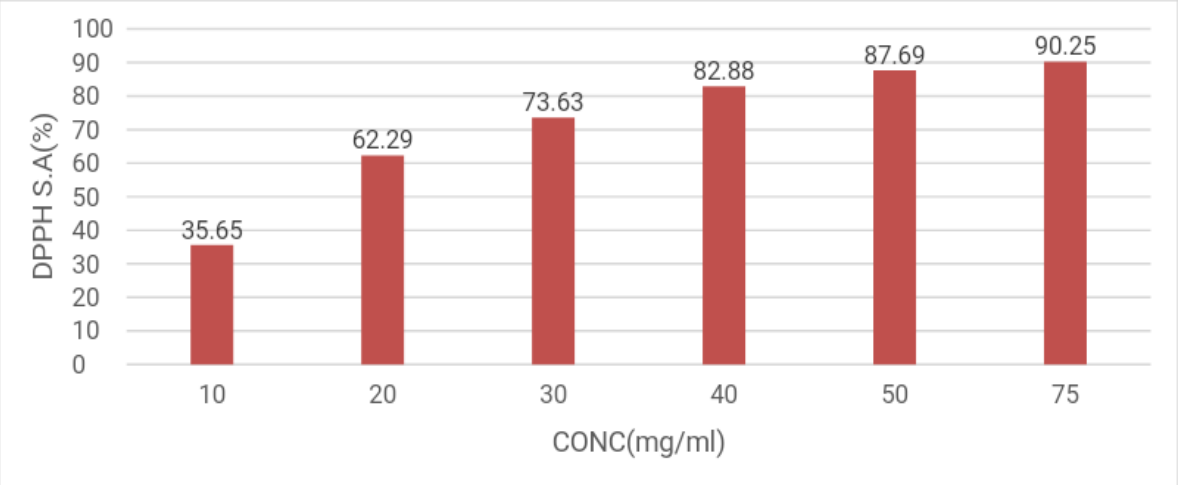

Fig. 7. Scavenging ability of leaves silver nanoparticles on DPPH

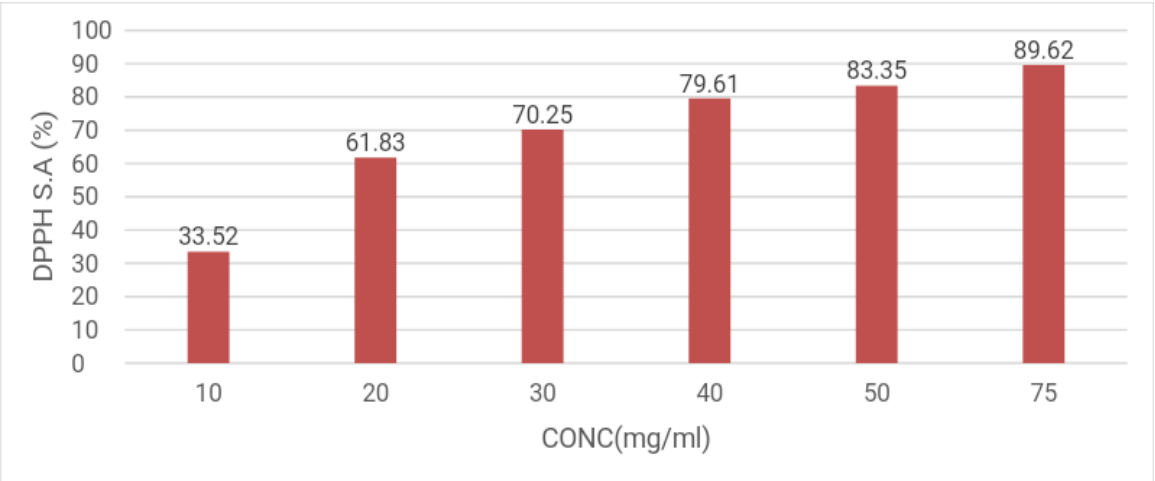

Fig. 8. Scavenging radical ability of leaves zinc nanoparticles on DPPH

For the zinc nanoparticles mediated from leaves extract of *V. subterranean,* the synthesized nanoparticles showed scavenging activity against DPPH at different concentrations of 10mg/ml (33.52%), 20mg/ml (61.83%), 30mg/ml (70.25%), 40mg/ml (79.61%), 50mg/ml (83.35%) and 75mg/ml (89.62%). The antioxidant activity was found to be higher as the concentration of the leaves extract zinc nanoparticles increased, with the highest activity 89.62% being at the concentration of 75mg/ml. The presence of the functional group in the phytochemicals present in the leaves of *V. subterranean* results in natural anti-oxidants with high reducing capacity [30]. The mechanism of anti-oxidant activity of silver nanoparticles was by single electron transfer to the DPPH radical; the silver nanoparticles have free radical resistive ability due to the antioxidant s in the nanoparticles. It is a possibility from the results obtained that the silver nanoparticles mediated from leaves extract possesses hydrogen-donating capabilities and acts as an antioxidant. This result is in support of the work conducted b Salve et.al. [28].

4. CONCLUSION

The aqueous leaves and roots extracts of the plant V. *subterranea*n was found suitable for the green synthesis of silver and zinc nanoparticles. The reduction of Ag^{+} to Ag^{0} resulted in the formation of the leaves nanoparticle that are spherical in shape having sizes within the range of 20 to 60nm, root nanoparticles that are rectangular in shape and size within the range of 55-85nm. The spectroscopic analysis using UV-vis spectroscopy show the nanoparticles had λ max absorption between 434 and 460nm in the visible region of the spectrum. The formation of amorphous nanoparticles and was confirmed by XRD studied which gave non-distinct diffraction peaks. Functional groups directly involved in the bio-reduction of silver and zinc ions to metallic silver and zinc nanoparticles were in the synthesized nano particles. The toxicity analysis showed that the synthesized nanoparticles have very low toxicity. The antimicrobial activity experiment performed on *Staphylococcus aureus* and *Salmonella typhi* demonstrated that the synthesized silver and zinc nanoparticles have antibacterial effects. These nanoparticles could find application in the therapy against disease caused by the bacterial species and others microorganisms. The anti-inflammatory analysis showed high activity for higher concentration and this means that the nanoparticles could find application in anti-inflammation therapy. The anti-oxidant activity conducted using DPPH showed significant scavenging activity at different concentrations. Further studies are recommended using younger immature leaves and this rsearch was conducted withIn conclusion, the leaves extract of *V. subterranean* was found to possess reasonable quantities of silver and zinc nanoparticles that exhibited antimicrobial, anti-inflammatory, antioxidant and free radical scavenging abilities. All these features were good health demands that have good application in today's modern medicine. There is need to conduct similar research using young immature leaves as this study utilized matured leaves discarded after harvest.

ACKNOWLEDGEMENT

The Authorsauthors wish to acknowledge the Tertiary Education Trust (TET) Fund and the management of Nnamdi Azikiwe University, Awka, for the award of the IBR grantsgrant which was utilized forin carrying out this research.

COMPETING INTERESTS

Authors have declared that no competing interests exist.

REFERENCES

1. Sadeghi B, Gholamhoseinpoor F. A study on the stability and green synthesis of silver nanoparticles using *Ziziphora tenuior* (Zt) extract at room temperature. Spectrochemical Acta Part Mol Biomol Spectrosc. 2015;134:310-5.
   DOI: 10.1016/j.saa.2014.06.046
2. Prathna TC, Chandrasekaran N, Ashok M, Raichur AM. Kinetic evolution study of silver nanoparticles in a bio-based green synthesis process. Colloids Surf A Physicochem Eng Aspects. 2011;377: 212-6.
3. Saifuddin N, Wong CW, Nuryasumira AA. Rapid biosynthesis of silver nanoparticles using culture supernatant of bacteria with microwave irradiation. E-journal of chemistry. 2009;6(1):61-70.
4. Feynman RP. There's plenty of room at the bottom. J Eng Sci. 1960;23(5):22-36.
5. Huang J, Li Q, Sun D. Biosynthesis of silver and gold nanoparticles by novel sundried Cinnamomum camphora leaf. J Nanotechnol. 2007;18(10).
6. Iravani S. Bacteria in nanoparticle synthesis current status and future prospects. Int Sch Res Not. 2014;20:1-18.

7. Mittal AK, Chisti Y, Banerjee UC. Synthesis of metallic nanoparticles using plant extracts. Biotechnol Adv. 2013;31(2): 346-56.
DOI: 10.1016/j.biotechadv.2013.01.003, PMID 23318667.
8. Mohanta YK, Bahera SK, Biosynthesis. characterization and antimicrobial activities of silver nanoparticles from *Cassia fistula* (Linn): in-vitro assessment of their antioxidant, antimicrobial and cytotoxic activities. IET Nanotechnol. 2016;10:438-44.
9. Nayak D, Pradhan S, Ashe S, Rauta PR, Nayak B. Biologically synthesized silver nanoparticles from three diverse family of plant extracts and their anticancer activities against epidermoid A421 carcinoma. J Colloid Interface Sci. 2015; 457:329-38.
DOI: 10.1016/j.jcis.2015.07.012
10. Santhoshkumar J, Sowmya B, Venkat Kumar S, Rajeshkumar S. Toxicological evaluation and antidermatophytic activity of silver nanoparticles synthesized using leaf extract of *Passifora caerulea*. S Afr J Chem Eng. 2019;29:17-23.
DOI: 10.1016/j.sajce.2019.04.001
11. Jain D, Daima HK, Kachhwala S, Kothari SL. Synthesis of plant-mediated silver nanoparticles using papaya fruit extract and evaluation of the antimicrobial activities. Digest Journal of Nanomaterials and Biostructure. 2009;4(3):557-63.
12. Hillocks RJ, Bennett C, Mponda OM. Bambara groundnut: A review of utilization, market potential and crop improvement. Afr Crop Sci J. 2012;20(1):1-16.
13. Anchirinah VM, Yiridoe EK, Bennett-Lartey SO. Enhancing sustainable production and genetics resources conservation of Bambara groundnut: A survey of indigenous agricultural knowledge system. Outlook Agric. 2001;30(4):281-8.
DOI: 10.5367/000000001101293788
14. 14Tan, Azam-Ali S, Goh EV, Mustafa M, Chai HH, Ho WK, Mayes S, et al. Bambara groundnut: An underutilized Leguminous Crop for Global food security and nutrition. Front Nutr. 2020;X. L:7.
DOI: 10.3389/fnut.2020.601496
15. 15.Adaora Stellamaris Ogbuagu, Okoye NNN, Innocent CL. *Vigna subterranean* (Bambara groundnut) a possible weapon in fighting the malnutrition war in arid and sub arid regions. World J Adv Res Rev. 2023;17(03):242-9.
16. Mayes S, Ho WK, Chai HH, Song B, Chang T, Massawe F. Bambara groundnut (*Vigna subterranean* (L) Verdc)- A climate smart crop for food and nutrition security. Genomic Designing of climate – smart pulse crops. 2019;397-424.
17. Paliwal R, Abberton M, Faloye B, Olaniyi O. Developing the role of legumes in West Africa under climate change. Curr Opin Plant Biol. 2020;56:242-58.
DOI: 10.1016/j.pbi.2020.05.002, PMID 32616362.
18. Manisha DR, Alwale J, Kudle KR, Pratap-Rudra MP. Biosynthesis of silver nanoparticles using flower extracts of Catharanthus roseus and evaluation of its antibacterial efficacy. World J Pharm Pharm Sci. 2014;3(5):877-85.
19. Abdulkadir MNJ, Safanah AF, Rasha MD. Green synthesis of silver nanoparticles using seed aqueous extract of Abelmoschus esculentus and study of their properties. Advances in Environmental9 biology. 2016;10(4):51-66.
20. Naseer M, Aslam U, Khalid B, Chen B. Green route to synthesize zinc oxide nanoparticles using leaf extracts of *Cassia fistula* and *Melia azedarach* and their antibacterial potential [scientific report]. Vol. 10; 2020. p. 9055-64.
21. Igwe OU, Nwamezie F. Green synthesis of iron nanoparticles using flower extract of *Pilliostigma thonningi* and their antibacterial activity evaluation. Chemistry International Journal. 2018;4(1):60-6.
22. Pratap MP, Manisha DR, Jahnavi A, Karunakor RK. Biosynthesis of silver nanoparticles using flower extracts of Catharanthus roseus and evaluation of its antibacterial efficacy. World J Pharm Pharm Sci. 2014;3(5):877-85.
23. Prakash P, Gnanaprakasam P, Emmanuel R, Arokiyaraj S, Saravanan P. Green synthesis of silver nanoparticles from leaf extract of *Mimusops elengi*, Linn for enhanced anti-bacterial activity against multi drug resistant clinical isolates. Colloids Surf B Biointerfaces. 2013;1(108):255-9.
24. Njagi EC, Huang H, Stafford L, Genuino H, Galindo HM, Collins JB, et al. Biosynthesis of iron and silver nanoparticles at room temperature using aqueous sorghum bran extracts. Langmuir. 2011;27(1):264-71.
DOI: 10.1021/la103190n, PMID 21133391.
25. Nadagouda MN, Castle AB, Murdock RC, Hussain SM, Varma RS. *In vitro*

biocompatibility of nanoscale zerovalent iron nanoparticles (NZVI) synthesized using tea polyphenol. Green Chem. 2010; 12(1):114-22.
DOI: 10.1039/B921203P

26. Hombach M, Maurer FP, Pfiffner T, Böttger EC, Furrer R. Standardization of operator-dependent variables affecting precision and accuracy of the disk diffusion method for antibiotic susceptibility testing. J Clin Microbiol. 2015;53(12):3864-9.
DOI: 10.1128/JCM.02351-15, PMID 26468500.
27. Ogbuagu AS, Maduka CC, Okerulu IO, Onyema CT, Onyeizugbe Chidi, Emezie UA. Comparative Nutritional and antimicrobial Screening of the Seed, Leaf and Root of *Vigna subterranean*. Prog. Chem Biochem Res. 2022;5(2): 182-95.
28. Salve P, Vinchurkar A, Raut R, Chondekar R, Lakkakula J, Roy A, et al. R. and Azlina, M.F. An evaluation of antimicrobial, anticancer, anti-inflammatory and antioxidant activities of silver nanoparticles synthesized from leaves extract of Madhula longifolia utilizing quantitative and qualitative methods. Molecules. 2022; 27(1):6404-19.
29. Rangasamy KS. Synthesis and characterization of silver nanoparticles from leaf extract of *Parthenuim hysterophorus* and antibacterial and antioxidant activity. Int J Curr Microbiol Appl Sci. 2013;2(6):220-7.
30. Naseer M, Aslam U, Khalid B, Chen B. Green route to synthesize nanoparticles using the leaf extract of *Cassia fistula* and *Melia azedarach* and their antibacterial potential. Sci Rep. 2020;10(9055):1-10.

Peer-review history:
The peer review history for this paper can be accessed here:
https://www.sdiarticle5.com/review-history/99172